TGA study examining the effect of pressure and peak temperature on biochar yield during pyrolysis of two-phase olive mill waste

Joan J. Manyà [a*], F. Xavier Roca [b], J. Francisco Perales [b]

[a] Thermo-chemical Processes Group (GPT), Aragón Institute of Engineering Research (I3A), University of Zaragoza, Mariano Esquillor s/n, E-50018 Zaragoza, Spain.

[b] Laboratori del Centre de Medi Ambient, Universitat Politècnica de Catalunya (LCMA-UPC), Avda. Diagonal, 647, E-08028 Barcelona, Spain

[*] Corresponding author: Joan J. Manyà. E-mail address: joanjoma@unizar.es. Fax: +34 974239302.

ABSTRACT

In this paper, a factorial design of experiments was proposed to investigate the effect of the absolute pressure (in the range 0.1–1.5 MPa) and the peak temperature (in the range 400–550 ºC) on the pyrolysis behaviour of two-phase olive mill wastes (TPOMW). Pyrolysis experiments were conducted in a thermogravimetric analyser (TGA) under nitrogen atmosphere and at a linear heating rate of 5 K min^{-1}. The response variables (biochar yield, fixed-carbon yield, and the temperature at which the maximum rate of weight loss is reached) were analysed using regression models. From results of regression analyses, the following main conclusions can be drawn: (a) biochar yield from pyrolysis of TPOMW decreases when both peak temperature and pressure increases; (b), an increase of both peak temperature and pressure results in a higher fixed-carbon yield; and (c), a significant increase of the overall devolatilisation rate was observed for experiments conducted at intermediate pressure values (0.8 MPa). In addition to this, kinetic parameters describing TPOMW pyrolysis were estimated adopting a devolatilisation scheme based on separate volatilised fractions generated from three pseudo-components. The quality of the fit between experimental weight-loss data and computed values (using an independent parallel reaction kinetic model) was found to be remarkably good.

Keywords: Biochar; Pyrolysis; Pressure; Two-phase olive mill waste; Response Surface Model; Kinetics.

1. Introduction

In recent years, an increasing number of research studies have highlighted the benefit of using *biochar* in terms of mitigating global warming and as a strategy to manage soil health and productivity [1–4]. Biochar is a carbon-rich, porous substance; which is produced by thermal decomposition of biomass under oxygen-limited conditions and at relatively low temperatures (< 700 °C) [1,5]. The definition adopted by the International Biochar Initiative (IBI) furthermore specifies the need for purposeful application of this material to soil for both agricultural and environmental gains [5]. In the case that biochar is obtained from a solid waste, an additional benefit linked to biochar strategy might be achieved: the valorisation of a lignocellulosic waste material generated from various industries, for example, food and forestry industries.

It is well known that the olive oil industry plays an important role in the Mediterranean countries' economy. Within these countries, Spain is the main producer with an average production of 0.9 10^6 metric tons per year [6,7]. In the last years, many Spanish manufacturers have implemented production processes based on a two-phase centrifugation system for both quality and environmental purposes [8,9]. This system involves two phases: a liquid phase (extra-virgin olive oil) and a solid (sludge) phase, which is called by different names: two-phase olive mill waste (TPOMW), "alperujo", or wet pomace [10]. TPOMW is an acidic and very-wet solid waste, the disposal of which is one of the main concerns for this type of food industry. Frequently, TPOMW is used as a soil amendment after a compositing process [11–13]. Alternatively, this type of waste can be pyrolysed for biochar or bio-oil purposes.

Conventional carbonisation or slow pyrolysis process is the most common way to generate biochar from a biomass feedstock. Pyrolysis involves a cracking process on polymeric structure to convert the biomass into charcoal and volatile matter. It is generally assumed that the charcoal yield is expected to increase as the heating rate becomes lower. For this reason, slow pyrolysis processes, in which the fuel material is heated at a rate usually ranged from 5 to 30 K min^{-1}, are preferred over other thermochemical processes for producing charcoal.

As a result of many previous studies focused on increasing charcoal yields [14–19], several factors that can play a key role during the pyrolysis process have been considered; among these are peak temperature, pressure, vapour residence time, and moisture content. Peak temperature is defined as the highest temperature value reached during the pyrolysis process [16]. As a general trend, the charcoal yield decreases as temperature increases. Nevertheless, an increase of peak temperature leads to an increasing content of fixed-carbon in the produced charcoal [16,20–21]. This effect is particularly pronounced in the temperature range from 300 to 500 ºC. On the other hand, pyrolysis under moderate pressure (0.5–3.0 MPa) seems to increase the charcoal yield due to the longer vapour residence time within the solid particle. This effect, which results in an increase of charcoal production due to the major role of secondary reactions (by means of which additional charcoal is produced by repolymerisation of volatile matter), seems to be more pronounced when the gas flow through the particle bed is small [16]. Regarding the potential effect of the moisture content of the biomass feedstock on pyrolysis results, previous studies [17,22] showed that moisture content can improve the yield of charcoal at pressures around 0.5–3.0 MPa. This finding makes some agricultural residues like olive mill wastes, which are characterised by high moisture contents, particularly attractive for biochar purposes.

Despite of the large number of studies published to date regarding charcoal from biomass, it should be noted that the estimation of the charcoal yield as a function of both operating conditions for a given biomass feedstock is still difficult. The specific aim of the present study is to analyse the effect of the absolute pressure (in the range 0.1–1.5 MPa) and the peak temperature (in the range 400–550 ºC) on the pyrolysis behaviour (charcoal yield, fixed-carbon yield, and apparent kinetics) of a TPOMW sample. The pyrolysis experiments were conducted in a thermogravimetric analyser (TGA) under nitrogen atmosphere and at a linear heating rate of 5 K min^{-1}. In order to assure the statistical significance of the observed effects, an unreplicated 2^k factorial design of experiments with the addition of 3 centre points was applied. The response variables (charcoal yield, fixed-carbon yield, and temperature at which maximum

devolatilisation rate is attained) as a function of the selected factors were analysed using Response Surface Methodology (RSM).

2. Materials and methods

2.1. Two-Phase olive mill waste sample

The sample of olive residue was taken from a factory located in the region of Aragón (Spain). In the factory, olive mill wastes are sun dried in the field for several months. Table 1 shows the results corresponding to the proximate and ultimate analyses for the raw material. Regarding the ash composition, the results of the X-ray fluorescence (XRF) analysis are shown in Table 2. A Thermo Electron ARL ADVANTXP+ XRF spectrometer was used to determine the ash compositions in terms of weight fractions of the main oxide constituents [23]. Olive residue was broken in a jaw crusher and sieved to obtain a particle size in the range of 250–500 μm.

2.2. TGA experiments

Experiments were conducted in a CAHN thermogravimetric analyser model TG-151 under a nitrogen atmosphere. An internal quartz tube (with an inner diameter of 34.5 mm) separates the reaction chamber from the furnace. The samples, with an initial mass of 160–190 mg, were placed inside a quartz sample pan. The N_2 flow through the reaction chamber was kept constant at 1.667 $cm^3\ s^{-1}$ (normal conditions). System pressure, in the range 0.1–2.5 MPa, is controlled by means of a back pressure regulator valve. A linear heating program, with a heating rate of 5 K min^{-1}, was chosen to heat the samples from room temperature to 110 ºC and from this value to the corresponding peak temperature value (in the range 400–550 ºC). Temperature was kept constant at 110 ºC for 60 min to ensure the complete drying. Final temperature was also kept constant during 120 min to achieve a stable final mass. The weight-loss curves were normalised by their sample mass value after the isothermal drying section (at 110 ºC during 60 min).

Relatively large sample masses were used in order to get representative results. This fact, however, may cause serious systematic errors in the measurement of the sample temperature.

Low initial sample masses (1–4 mg) are commonly used in thermogravimetry to avoid the effect of transport phenomena [24–25]. Nevertheless, the use of small sample sizes can lead to other potential problems, such as the inability to asses a representative and unbiased sample and, additionally, the possibility to magnify surface reactions at the expense of intra-bed controlling processes [24].

2.3. Experimental design

The TGA runs were performed according to an unreplicated two-level factorial design. The levels of the investigated factors (pressure and peak temperature) are given in Table 3. It is well known that a feasible method to estimate the intrinsic experimental error is the addition of several centre points (3 replicates in the present study) to the 2^k design [26]. Moreover, the inclusion of centre points allows the estimation of the curvature, due to pure quadratic effects [27].

Three response variables have been analysed: the char yield (y_{char}), the yield of fixed-carbon (y_{FC}), and the temperature of maximum rate of devolatilisation (T_{max}).

The fixed carbon yield is considered a better index than the charcoal yield, because the y_{FC} takes into account the chemical composition of the produced charcoal [21]. This index is defined as follows:

$$y_{FC} = \left(\frac{m_{char}}{m_{bio}}\right)\left(\frac{\%FC}{100-\%ash}\right) \quad (1)$$

where *%FC* and *%ash* correspond to the percentage of fixed-carbon contained in the charcoal and the percentage of ash in the feedstock, respectively. The ratio between m_{char} (mass of produced charcoal after 120 min at the given peak temperature) and m_{bio} (dry mass of feedstock after 60 min at 110 ºC) is the charcoal yield (y_{char}).

Concerning T_{max}, the temperature at which the maximum rate of weight loss is reached, its value corresponds to the overall maximum of the sign-changed derivative mass-loss curve (–DTG curve) and is closely related to the devolatilisation reactivity of the solid fuel.

For both the factorial design of experiments and its statistical analysis, the RcmdrPlugin.DoE package [28] within R environment (version 2.14.2) was used.

3. Results and discussion

In this section, experimental results for the response variables are presented and discussed. In addition, the results of the parameters estimation and the performance of an independent parallel reaction (IPR) kinetic model are also provided.

3.1. Accuracy of the experimental data

Repeatability, or variability due to the measuring device, was analysed from the three measuring tests corresponding to the centre points. For this purpose, a crossed gauge R&R study (using the ANOVA method) [29] was conducted within R environment. A hundred of measurements of the standardised mass, the ratio between the experimental mass at a given time (m_t) and the dry mass of feedstock after 60 min at 110 ºC (m_{bio}), at the same experimental time (and temperature) for the three replicates were evaluated. The final results of the gauge R&R study indicated that the contribution to the total variance due to the repeatability of measurement equipment was 18.94%, whereas the contribution of part-to-part, as expected, was dominant (81.06%). In addition, it should be kept in mind that the variability due to the equipment could mainly be attributed to external sources of uncertainty, such as sample heterogeneity and initial sample mass. On the other hand; Figure 1 shows the comparison of the TGA weight-loss curves for the replicated centre point data. From visual inspection of this figure and taking into account the results of the above-mentioned gauge R&R study, it seems reasonable to assume that there are not large variations among replicates. Finally, it should be highlighted that the value of the dried initial mass (m_{bio}), which was different in replicate experiments (141.35, 132.79, and 127.27 mg), does not cause any significant shift of the TGA curve. This finding is consistent with the results reported by Stenseng and co-workers [30] and Jumpirom and co-workers [31],

who observed that the effect of the initial sample mass did not affected the heat transfer resistance during biomass pyrolysis at low heating rate conditions (40 K min^{-1} or less).

3.2. Analysis of response variables

The two factors were screened by means of an unreplicated full factorial design with 3 replicates at the centre point to make a total of 7 runs. Analysis of variance (ANOVA) was performed on experimental data (which is reported in Table 4) assuming a significance level (α) of 0.05. In this way, coefficients having *p*-values less than 0.05 are considered statistically significant.

For the charcoal yield, Table 5 shows the summary of the linear regression model. The fitted model, expressed in terms of coded variables [–1,+1], is given below:

$$y_{char} = 0.3446 - 0.0344x_1 - 0.0436x_2 - 0.0094x_1x_2 \quad (2)$$

Figure 2 shows the contour plot corresponding to the above described model. The coefficient for the interaction term was not statistically significant (*p*-value = 0.377). The adjusted coefficient of determination (R^2_{adj}) value was 0.8556 and indicated that 88.56% of the total variation in the charcoal yield was attributed to the factors analysed. However, the *p*-value for the lack-of-fit test evidences that curvature is significant. In other words, a pure quadratic regression model seems to be more appropriate than the linear one. Nevertheless, the estimation of the quadratic coefficients is not possible without expanding the current two-level factorial design to a central composite design.

Regarding the fixed-carbon yield, Table 6 displays the regression coefficients and the ANOVA results for the following linear model:

$$y_{FC} = 0.2289 + 0.0034x_1 + 0.0044x_2 + 0.0017x_1x_2 \quad (3)$$

As observed for the previous response variable, the coefficient for the interaction term was not statistically significant (*p*-value = 0.242), whereas the result of the lack-of-fit test shows that

curvature is statistically significant (p-value = 0.035). Figure 3 shows the contour plot corresponding to model given by equation 3.

In the case of the temperature of maximum rate of devolatilisation (T_{max}) , linear regression including the interaction term was absolutely inaccurate (p-value of the F test equal to 0.991). Assuming that the curvature term is only explained by factor A (pressure), a pure quadratic regression model, which is given in equation 4, was fitted to the data (see Table 7 for statistical summary).

$$T_{\max} = 291.0 - 3.50x_1 - 1.5x_2 - x_1x_2 + 34.0x_1^2 \quad (4)$$

From the model showed above, it should be noted the inclusion of the curvature term allows the model to explain a 99.71% of the variability that is present in the data. Figure 4 displays the contour plot corresponding to model given by equation 4.

For all of the regression models developed in this research, the residuals were normally distributed as shown in the corresponding normal Q-Q plots (see Fig. 5). In addition to this, both residuals against predicted values and residuals against run number plots suggested a homogeneous variance.

The results of the regression analysis for the y_{char} response variable indicate that an increase of both peak temperature and pressure leads to a decrease of charcoal yield (see contour plot in Fig. 2). The effect of the peak temperature is in perfect agreement with most previous observations: see, for instance, the findings of Di Blasi and co-workers [14], González and co-workers [32], Mulligan and co-workers [33], and Duman and co-workers [34]. However, the sign of effect attributed to absolute pressure on charcoal yield was absolutely unexpected, since earlier studies indicated that pressure favours the charcoal production [17,21,35]. Antal and Gronli [16], after reviewing the state of the charcoal production science up to 2003, suggested that pressure prologues the residence time of tar vapours and, consequently, the formation of secondary carbon via the decomposition of vapours onto the carbonaceous matrix is enhanced. Obviously, this effect is pronounced when the gas flow rate through the particle bed is very small. At this

point, the authors would like to emphasise that, for experiments performed at pressures higher than atmospheric, the velocity of nitrogen through the reaction chamber was relatively low (0.4395 cm s^{-1} at 673 K and 0.1 MPa, and 0.02931 cm s^{-1} at 673 K and 1.5 MPa) resulting in relatively high gas residence times (1.89 min at 673 K and 0.1 MPa, and 28.4 min at 673 K and 1.5 MPa). However, the mass of biomass per volume of reactor in the TGA system is very low compared to a packed-bed reactor and, consequently, the diffusion of tar vapours through the particle bed can be achieved in a relatively easy way. Recently, Melligan and co-workers [36] reported that the effect of pressure (in the range 0.1–2.6 MPa) on the charcoal yield during the slow pyrolysis of miscanthus in a laboratory-scale fixed bed was negligible. This last finding is more in line with the results reported here. In any case, in further studies special attention should be focused on examining the effect of pressure on charcoal yield at different gas residence times for different reactor configurations.

Concerning the y_{FC} response variables, it should be noted that the statistically significant effects are not of great magnitude. Nevertheless, the behaviour of the dependent variable as a function of the factors is consistent with previous results, in which an increase of the fixed-carbon yield with the increase of both peak temperature [19,33,37–38] and pressure [17] were observed (see contour plot in Fig. 3).

Regarding T_{max}, Fig. 4 shows that curvature is evident and that the lowest T_{max} value is obtained when pressure was fixed at medium level (0.8 MPa). This finding suggests that pressure can have a serious effect on the kinetics of the overall devolatilisation process. For this reason, an additional kinetic study is presented in the next section.

3.3. Kinetic study

Mass loss data from the TGA experiments can be expressed as a function of conversion, which is defined as follows:

$$\alpha = \frac{m_{bio} - m_t}{m_{bio} - m_{char}} \tag{5}$$

where m_{bio} is the initial mass of sample (the dry mass of feedstock after 60 min at 110 ºC), m_t is the actual sample mass, and m_{char} is the residual mass after pyrolysis (mass of produced charcoal after 120 min at the given peak temperature). The conversion represents the mass fraction of sample which was decomposed.

The use of reaction-order models is very usual in the thermal analysis of biomass because of their simplicity [24,39]. In these models, the reaction rate is proportional to the fraction of undecomposed material raised to a specific exponent, which is known as the reaction order (n):

$$\frac{d\alpha}{dT} = k(T)(1-\alpha)^n \tag{6}$$

where $k(T)$ is the rate constant and obeys the Arrhenius equation:

$$k(T) = A\exp\left(\frac{-E}{RT}\right) \tag{7}$$

with A and E being the pre-exponential factor and the activation energy, respectively.

On the other hand, a devolatilisation scheme based on separate volatilised fractions generated from several pseudo-components has widely been adopted by the research community to describe apparent kinetics of biomass pyrolysis [15–16,40–43]. In the present study, it was assumed that the overall decomposition of the samples can be expressed as the sum of the volatiles formed from three-pseudo-components: hemicellulose (first pseudo-component), the major fraction of cellulose (second pseudo-component) and, as a third pseudo-component, the sum of lignin, the remaining fraction of cellulose, and other organic components. By adopting this approach, the pyrolysis rate can be expressed as follows:

$$\frac{d\alpha}{dt} = \beta\frac{d\alpha}{dT} = \sum_{i=1}^{3} c_i A_i \exp\left(\frac{-E_i}{RT}\right)(1-\alpha_i)^{n_i} \tag{8}$$

here c_i represents the contribution of the ith partial reaction to the overall weight loss, whereas β corresponds to the linear heating rate (5 K min^{-1} in this study).

The methodology followed to estimate the kinetic parameters from the experimental TGA curves is described in the following text. For a given thermogravimetric experiment, normalised mass (m_t/m_{bio}) was differentiated with respect the time to obtain the experimental values of decomposition rate. The normalised –DTG curve as a function of time was deconvoluted into three Gaussian distributions using the *Peak Analyser* tool within OriginPro v. 8.5 (OriginLab Corporation, USA). Each individual adjusted Gaussian peak, which represents the estimated values of $d\alpha_i/dt$ was then subjected to a non-linear least square (NLLS) fitting process by the Levenberg-Marquardt method [44], which is also implemented in OriginPro. As a result of this fitting process, estimated values for the parameters A_i, E_i, and n_i were obtained. Regarding the estimation of c_i parameters, their values were determined as the value of the integral of the Gaussian peak ($d\alpha_i/dt$) over the entire run time.

Table 8 shows, for all experiments performed, the estimated kinetic parameters and several statistical indicators of the goodness of fit, which are the adjusted coefficient of determination (R^2_{adj}) values obtained from the peak deconvolution procedure and from the non-linear lest square fitting processes conducted for each pseudo-component. The fit quality of a given experiment was calculated according to the following expression [45]:

$$fit(\%) = 100\frac{\sqrt{S}}{h_{\max}} \tag{9}$$

where S corresponds to the mean squared difference between the calculated and observed values of $d\alpha/dt$ and h_{max} equals to the maximum value of the experimental normalised –DTG curve. Note that lower fit values indicate better fit qualities. Figure 6 gives an example of the quality of the curve fitting.

For the experiments performed at atmospheric pressure, the values of the estimated activation energies for the three pseudo-components are generally within the range reported in many previous studies focused on gaining knowledge of the kinetics of biomass pyrolysis [24]. Nevertheless, it should be kept in mind that the above-mentioned range of data is extremely wide

(from 11.2 to 293.5 kJ mol^{-1}), as reported by White and co-workers [24]. This great variability can be explained by the fact that different biomass samples from various origins (with very variable composition and inorganic matter contents), different experimental conditions (sample mass, heating rate, thermogravimetric device, etc.), different kinetic models, and different parameter estimation approaches were used and/or adopted in the numerous previous studies.

Regarding the effect of pressure on the overall devolatilisation rate, Figure 7 compares the normalised –DTG curves for three experiments conducted at different pressures (run #5 at 0.1 MPa, run #1 at 0.8 MPa, and run #6 at 1.5 MPa). The shape of the –DTG curves visually confirms the effect of pressure on pyrolysis kinetics previously deduced from examining the response surface model. In addition, the values listed in Table 8 for the kinetic parameters of the second pseudo-component are in agreement with the previously mentioned behaviour of T_{max} as a function of pressure. In fact, the activation energy values were apparently lower for experiments conducted at the intermediate pressure level (0.8 MPa) than those for experiments carried out at both low and high pressure levels (0.1 MPa and 1.5 MPa, respectively). In order to statistically compare and contrast the E values obtained from data collected at different pressures, a Wilcoxon rank-sum test was performed for the two groups of experiments (those conducted at 0.8 MPa and those performed at a different pressure). This non-parametric test is more appropriate than the two-sample t-test when the sample size is small, and, consequently, normality assumption becomes uncertain. The results of the Wilcoxon test produce a p-value of 0.05714, indicating that the estimated values of activation energies are not significantly different at a significance level, α, of 0.05. However, the p-value is just slightly greater than 0.05, so there is some evidence that null hypothesis cannot be rejected.

4. Conclusions

In the present work, the effect of both the absolute pressure (in the range 0.1–1.5 MPa) and the peak temperature (in the range 400–550 ºC) on the pyrolysis of two-phase olive mill waste was analysed. Below is an itemised list of major conclusions and findings obtained.

- Biochar yield from pyrolysis of TPOMW decreases when both peak temperature and pressure increases.
- The unexpected effect of pressure on biochar yield could be due to the poor contact between the tar vapours and the solid sample in a TGA system. For this reason, additional studies are needed to confirm or contrast these findings. In this sense, further experimental studies should consider the gas residence time and other variables affecting the diffusivity of the vapour fraction (such as particle size and sample mass) as additional factors.
- An increase of both peak temperature and pressure results in a higher fixed-carbon yield. In other words, working at a pressure of 1.5 MPa and at a peak temperature of 550 °C is better from a process efficiency point of view.
- From analysing the response surface model for the T_{max} response variable, a significant increase of the devolatilisation rate was observed at intermediate pressure values (0,8 MPa). In this sense, the values of the estimated kinetic parameters confirm this behaviour.
- Further studies focused on analysing the effect of pressure for a narrow range (i.e., 0.1–5.0 MPa) are required in the near future to objectively assess the role of pressure in biomass pyrolysis. For this purpose, the use of central composite designs will be required to perform the calculations needed for fitting quadratic regression models.

Acknowledgements

J.J.M. gratefully acknowledges the financial support from Spain's State Secretariat for Research (Project ENE2011-22657).

References

[1] J. Lehmann, S. Joseph, Biochar for Environmental Management: An Introduction, in: J. Lehmann, S. Joseph (Eds.), Biochar for Environmental Management: Science and Technology, Earthscan, London, 2009, pp. 1-10.

[2] B. Glaser, J. Lehmann, W. Zech, Ameliorating physical and chemical properties of highly weathered soils in the tropics with charcoal – a review, Biol. Fertil. Soils 35 (2002) 219-230.

[3] A.D. Laird, The charcoal Vision: A win-win-win scenario for simultaneously producing bioenergy, permanently sequestering carbon, while improving soil and water quality, Agron. J. 100 (2008) 178-181.

[4] J.J. Manyà, Pyrolysis for biochar purposes: a review to establish current knowledge gaps and research needs, Environ. Sci. Technol 46 (2012) 7939-7954.

[5] S. Sohi, E. Lopez-Capel, E. Krull, R. Bol, Biochar, climate change and soil: A review to guide future research, CSIRO Land and Water Science Report 05/09 (2009) 1-56.

[6] IOOC (International Olive Oil Council), Annual Statistics of International Olive Oil Council. URL: http://www.internationaloliveoil.org (2004).

[7] B. Lozano-García, L. Parras-Alcántara, del Toro Carrillo de Albornoz,M., Effects of oil mill wastes on surface soil properties, runoff and soil losses in traditional olive groves in southern Spain, Catena 85 (2011) 187-193.

[8] M.L. Cayuela, P.D. Millner, S.L.F. Meyer, A. Roig, Potential of olive mill waste and compost as biobased pesticides against weeds, fungi, and nematodes, Sci. Total Environ. 399 (2008) 11-18.

[9] G. Tortosa, J.A. Alburquerque, G. Ait-Baddi, J. Cegarra, The production of commercial organic amendments and fertilisers by composting of two-phase olive mill waste ("alperujo"), J. Clean. Prod. 26 (2012) 48-55.

[10] A. Roig, M.L. Cayuela, M.A. Sánchez-Monedero, An overview on olive mill wastes and their valorisation methods, Waste Manage. 26 (2006) 960-969.

[11] J.A. Alburquerque, J. Gonzalvez, D. Garcia, J. Cegarra, Effects of bulking agent on the composting of "alperujo", the solid by-product of the two-phase centrifugation method for olive oil extraction, Process Biochem. 41 (2006) 127-132.

[12] L. Ruggieri, E. Cadena, J. Martinez-Blanco, C.M. Gasol, J. Rieradevall, X. Gabarrell, T. Gea, X. Sort, A. Sanchez, Recovery of organic wastes in the Spanish wine industry. Technical, economic and environmental analyses of the composting process, J. Cleaner Prod. 17 (2009) 830-838.

[13] I.S. Arvanitoyannis, T.H. Varzakas, Vegetable waste treatment: Comparison and critical presentation of methodologies, Crit. Rev. Food Sci. Nutr. 48 (2008) 205-247.

[14] C. Di Blasi, G. Signorelli, C. Di Russo, G. Rea, Product Distribution from Pyrolysis of Wood and Agricultural Residues, Ind. Eng. Chem. Res. 38 (1999) 2216-2224.

[15] J.J. Manyà, J. Ruiz, J. Arauzo, Some peculiarities of conventional pyrolysis of several agricultural residues in a packed bed reactor, Ind Eng. Chem. Res. 46 (2007) 9061-9070.

[16] M.J. Antal, M. Gronli, The Art, Science, and Technology of Charcoal Production, Ind. Eng. Chem. Res. 42 (2003) 1619-1640.

[17] M.J. Antal, E. Croiset, X. Dai, C. DeAlmeida, W.S. Mok, N. Niclas, J.R. Richard, M. Al Majthoub, High-Yield Biomass Charcoal, Energy Fuels 10 (1996) 652-658.

[18] G. Varhegyi, P. Szabo, F. Till, B. Zelei, M.J. Antal, X. Dai, TG, TG-MS, and FTIR Characterization of High-Yield Biomass Charcoals, Energy Fuels 12 (1998) 969-974.

[19] A. Demirbas, Effects of temperature and particle size on bio-char yield from pyrolysis of agricultural residues, J. Anal. Appl. Pyrolysis 72 (2004) 243-248.

[20] Y. Schenkel, P. Bertaux, S. Vanwijnbserghe, J. Carre, An evaluation of the mound kiln carbonization technique, Biomass Bioenergy 14 (1998) 505-516.

[21] M.J. Antal, S.G. Allen, X. Dai, B. Shimizu, M.S. Tam, M. Gronli, Attainment of the Theoretical Yield of Carbon from Biomass, Ind. Eng. Chem. Res. 39 (2000) 4024-4031.

[22] G. Várhegyi, P. Szabó, W.S. Mok, M.J. Antal, Kinetics of the thermal decomposition of cellulose in sealed vessels at elevated pressures. Effects of the presence of water on the reaction mechanism, J. Anal. Appl. Pyrolysis 26 (1993) 159-174.

[23] C. Liao, C. Wu, Y. Yan, The characteristics of inorganic elements in ashes from a 1 MW CFB biomass gasification power generation plant, Fuel Process Technol. 88 (2007) 149-156.

[24] J.E. White, W.J. Catallo, B.L. Legendre, Biomass pyrolysis kinetics: A comparative critical review with relevant agricultural residue case studies, J. Anal. Appl. Pyrolysis 91 (2011) 1-33.

[25] G. Varhegyi, B. Bobaly, E. Jakab, H. Chen, Thermogravimetric Study of Biomass Pyrolysis Kinetics. A Distributed Activation Energy Model with Prediction Tests, Energy Fuels 25 (2011) 24-32.

[26] D.C. Montgomery, Design and Analysis of Experiments, 6th ed., John Wiley & Sons, Hoboken, NJ, 2005.

[27] K.M. Isa, S. Daud, N. Hamidin, K. Ismail, S.A. Saad, F.H. Kasim, Thermogravimetric analysis and the optimisation of bio-oil yield from fixed-bed pyrolysis of rice husk using response surface methodology (RSM), Ind. Crops Prod. 33 (2011) 481-487.

[28] U. Groemping, RcmdrPlugin.DoE: R Commander Plugin for (industrial) Design of Experiments, version 0.11-5, URL: http://cran.r-project.org/web/packages/RcmdrPlugin.DoE/index.html (2012).

[29] R.K. Burdick, C.M. Borror, D.C. Montgomery, Design and Analysis of Gauge R&R Studies: Making Decisions with Confidence Intervals in Random and Mixed ANOVA Models, ASA-SIAM Series on Statistics and Applied Probability, Philadelphia, PA, 2005.

[30] M. Stenseng, A. Jensen, K. Dam-Johansen, Investigation of biomass pyrolysis by thermogravimetric analysis and differential scanning calorimetry, J Anal. Appl. Pyrolysis 58-59 (2001) 765-780.

[31] S. Junpirom, C. Tangsathitkulchai, M. Tangsathitkulchai. Thermogravimetric analysis of longan seed biomass with a two-parallel reactions model, Korean J. Chem. Eng. 27 (2010) 791-801.

[32] J.F. González, J.M. Encinar, J.L. Canito, E. Sabio, M. Chacón, Pyrolysis of cherry stones: energy uses of the different fractions and kinetic study, J. Anal. Appl. Pyrolysis 67 (2003) 165-190.

[33] C.J. Mulligan, L. Strezov, V. Strezov, Thermal Decomposition of Wheat Straw and Mallee Residue Under Pyrolysis Conditions, Energy Fuels 24 (2010) 46-52.

[34] G. Duman, C. Okutucu, S. Ucar, R. Stahl, J. Yanik, The slow and fast pyrolysis of cherry seed, Bioresour. Technol. 102 (2011) 1869-1878.

[35] M.J. Antal, W.S. Mok, G. Varhegyi, T. Szekely, Review of Methods for Improving the Yield of Charcoal from Biomass, Energy Fuels 4 (1990) 221-225.

[36] F. Melligan, R. Auccaise, E.H. Novotny, J.J. Leahy, M.H.B. Hayes, W. Kwapinski, Pressurised pyrolysis of Miscanthus using a fixed bed reactor, Bioresour. Technol. 102 (2011) 3466-3470.

[37] J.F. Gonzalez, A. Ramiro, C.M. Gonzalez-Garcia, J. Gañan, J.M. Encinar, E. Sabio, J. Rubiales, Pyrolysis of Almond Shells. Energy Applications of Fractions, Ind. Eng. Chem. Res. 44 (2005) 3003-3012.

[38] F. Karaosmanoglu, A. Isigigur-Ergundenler, A. Sever, Biochar from the Straw-Stalk of Rapeseed Plant, Energy Fuels 14 (2000) 336-339.

[39] A. Khawam, D.R. Flanagan, Solid-state kinetic models: basics and mathematical fundamentals, J. Phys. Chem. B 110 (2006) 17315-17328.

[40] Y. Park, J. Kim, S. Kim, Y. Park, Pyrolysis characteristics and kinetics of oak trees using thermogravimetric analyzer and micro-tubing reactor, Bioresour. Technol. 100 (2009) 400-405.

[41] E. Biagini, A. Fantei, L. Tognotti, Effect of the heating rate on the devolatilization of biomass residues, Thermochim. Acta. 472 (2008) 55-63.

[42] K.G. Santos, F.S. Lobato, T.S. Lira, V.V. Murata, M.A.S. Barrozo, Sensitivity analysis applied to independent parallel reaction model for pyrolysis of bagasse, Chem. Eng. Res. Design (2012), http://dx.doi.org/10.1016/j.cherd.2012.04.007.

[43] S. Hu, A. Jess, M. Xu, Kinetic study of Chinese biomass slow pyrolysis: Comparison of different kinetic models, Fuel 86 (2007) 2778-2788.

[44] A. Bjorck, Numerical methods for least squares problems, SIAM, Philadelphia, PA, 1996.

[45] M. Trninić, L. Wang, G. Várhegyi, M. Grønli, Ø. Skreiberg, Kinetics of Corncob Pyrolysis, Energy Fuels 26 (2012) 2005-2013.

Nomenclature

A: Pre-exponential factor of the Arrhenius equation (s^{-1}).

c_i: Contribution of the ith pseudo-component to the overall weight loss.

E: Activation energy (J mol^{-1}).

h_{max}: Maximum value of the experimental normalised –DTG curve.

m_{bio}: Dry mass of feedstock after 60 min at 110 ºC (mg).

m_{char}: Mass of produced charcoal after 120 min at the given peak temperature (mg).

m_t: Actual sample mass as a function of experimental time (mg).

n: Reaction order.

p: Absolute pressure (MPa)

T_{max}: Temperature at which the maximum rate of weight loss is reached (°C).:

T_{peak}: Peak temperature (°C).

x: Coded variable (in the range from –1 to 1) of the regression model.

y_{char}: Char yield.

y_{FC}: Fixed carbon yield.

Greek symbols

α: Conversion of the overall devolatilisation process.

β: Linear heating rate (K min^{-1}).

Acronyms

RSM: Response surface methodology (or model).

TGA: Thermogravimetric analysis.

TPOMW: Two-phase oil mill waste.

XRF: X-ray fluorescence.

Table 1

Proximate and Elemental analyses of TPOMW samples.

Proximate	Analytical standard	% by weight	*Ultimate (organic fraction)*	Analytical instrument	% by weight (daf*)
Moisture	ISO-589-1981	16.85	Carbon	Carlo Erba 1108	49.47
Ash	ISO-1171-1976	2.27	Hydrogen		6.01
Volatile	ISO-5623-1974	63.61	Nitrogen		0.44
Fixed Carbon	By difference	17.27	Sulphur		0.10
			Chlorine		0.08

* Dry and ash-free basis

Table 2

Ash elemental analysis of TPOMW samples (expressed as percentage of oxides by weight).

	CaO	K_2O	SiO_2	Fe_2O_3	Al_2O_3	P_2O_5	MgO	TiO_2	PbO	SnO2	CuO	MnO	ZnO	SrO	S_{inorg}	Cl
Ash basis (%)	42.1	26.4	10.0	6.90	3.91	3.90	1.69	0.476	0.256	0.231	0.221	0.196	0.137	0.084	2.95	0.251

Table 3

Analysed factors and their levels.

Level	Factors	
	A	B
	Pressure (MPa)	Peak Temperature (ºC)
Low (–1)	0.10	400
Centre (0)	0.8	475
High (+1)	1.5	550

Table 4

Experimental data for the two-level factorial design.

Run	p (MPa)	T_{peak} (ºC)	y_{char}	y_{FC}	T_{max} (ºC)
1	0.8	475	0.3613	0.2275	292
2	1.5	550	0.2471	0.2397	319
3	0.10	550	0.3347	0.2295	328
4	0.8	475	0.3535	0.2264	291
5	0.10	400	0.4031	0.2240	329
6	1.5	400	0.3530	0.2275	324
7	0.8	475	0.3594	0.2278	290

Table 5

Regression coefficients and ANOVA table for the regression model (response variable: y_{char}).

```
Coefficients:
             Estimate Std. Error t value Pr(>|t|)
(Intercept)  0.344586   0.006856  50.258 1.73e-05 ***
x1          -0.034425   0.009070  -3.795   0.0321 *
x2          -0.043575   0.009070  -4.804   0.0172 *
x1:x2       -0.009375   0.009070  -1.034   0.3773
---
Signif. codes:  0 '***' 0.001 '**' 0.01 '*' 0.05 '.' 0.1 ' ' 1

Residual standard error: 0.01814 on 3 degrees of freedom
Multiple R-squared: 0.9278,     Adjusted R-squared: 0.8556
F-statistic: 12.85 on 3 and 3 DF,  p-value: 0.03221

Analysis of Variance Table

Response: ychar
            Df    Sum Sq   Mean Sq F value  Pr(>F)
FO(x1, x2)   2 0.0123354 0.0061677 18.7431 0.02017
TWI(x1, x2)  1 0.0003516 0.0003516  1.0684 0.37733
Residuals    3 0.0009872 0.0003291
Lack of fit  1 0.0009541 0.0009541 57.6736 0.01690
Pure error   2 0.0000331 0.0000165
```

Table 6

Regression coefficients and ANOVA table for the regression model (response variable: y_{FC}).

```
Coefficients:
             Estimate Std. Error t value Pr(>|t|)
(Intercept) 0.2289143  0.0008707 262.904 1.21e-07 ***
x1          0.0034250  0.0011518   2.973   0.0589 .
x2          0.0044250  0.0011518   3.842   0.0311 *
x1:x2       0.0016750  0.0011518   1.454   0.2419
---
Signif. codes:  0 '***' 0.001 '**' 0.01 '*' 0.05 '.' 0.1 ' ' 1

Residual standard error: 0.002304 on 3 degrees of freedom
Multiple R-squared: 0.8955,     Adjusted R-squared: 0.791
F-statistic: 8.572 on 3 and 3 DF,  p-value: 0.0555

Analysis of Variance Table

Response: yFC
             Df     Sum Sq    Mean Sq F value  Pr(>F)
FO(x1, x2)    2 1.2525e-04 6.2622e-05 11.7999 0.03788
TWI(x1, x2)   1 1.1222e-05 1.1222e-05  2.1147 0.24187
Residuals     3 1.5921e-05 5.3070e-06
Lack of fit   1 1.4834e-05 1.4834e-05 27.3026 0.03473
Pure error    2 1.0870e-06 5.4300e-07
```

Table 7

Regression coefficients and ANOVA table for the regression model (response variable: T_{max}).

```
Coefficients: (1 not defined because of singularities)
              Estimate Std. Error t value Pr(>|t|)
(Intercept)   291.0000     0.5774  504.03 3.94e-06 ***
FO(x1, x2)1    -3.5000     0.5000   -7.00 0.019804 *
FO(x1, x2)2    -1.5000     0.5000   -3.00 0.095466 .
TWI(x1, x2)    -1.0000     0.5000   -2.00 0.183503
PQ(x1, x2)1^2  34.0000     0.7638   44.52 0.000504 ***
PQ(x1, x2)2^2       NA         NA      NA       NA
---
Signif. codes:  0 '***' 0.001 '**' 0.01 '*' 0.05 '.' 0.1 ' ' 1

Residual standard error: 1 on 2 degrees of freedom
Multiple R-squared: 0.999,      Adjusted R-squared: 0.9971
F-statistic: 510.9 on 4 and 2 DF,  p-value: 0.001954
```

Table 8

List of the kinetic parameters estimated from thermogravimetric experiments.

Run	p (MPa)	T_{peak} (ºC)	R^2_{adj} of peak fit	Kinetic parameters: A_i (s^{-1}); E_i (J mol^{-1}); n_i.	R^2_{adj} of NLLS fit	T_{max} for the calculated peaks(ºC)	Contribution to the weight loss (c_i)	Fit (%)
5	0.1	400	0.9943	$A_1 = 7.6544\ 10^6 \pm 3.3387\ 10^6$ $E_1 = 106381 \pm 2048$ $n_1 = 1.366 \pm 0.023$	0.9960	280	0.2222	2.12
				$A_2 = 7.8337\ 10^{11} \pm 2.2746\ 10^{11}$ $E_2 = 173118 \pm 15533$ $n_2 = 0.877 \pm 0.065$	0.9431	328	0.1401	
				$A_3 = 4.9730 \pm 0.4352$ $E_3 = 49660 \pm 438$ $n_3 = 1.242 \pm 0.010$	0.9984	341	0.2388	
3	0.1	550	0.9972	$A_1 = 1.7964\ 10^7 \pm 9.5684\ 10^6$ $E_1 = 109976 \pm 2510$ $n_1 = 1.279 \pm 0.025$	0.9952	280	0.2207	1.34
				$A_2 = 3.0755\ 10^{11} \pm 8.4716\ 10^{10}$ $E_2 = 167445 \pm 14631$ $n_2 = 1.037 \pm 0.071$	0.9458	327	0.1616	
				$A_3 = 0.1093 \pm 0.0035$ $E_3 = 33105 \pm 155$ $n_3 = 1.139 \pm 0.051$	0.9996	364	0.2805	
1	0.8	475	0.9905	$A_1 = 1.7483\ 10^9 \pm 1.5323\ 10^8$ $E_1 = 120518 \pm 3882$ $n_1 = 1.223 \pm 0.034$	0.9910	239	0.1901	2.70
				$A_2 = 1.8801\ 10^{10} \pm 2.8741\ 10^9$ $E_2 = 143346 \pm 7526$ $n_2 = 1.059 \pm 0.047$	0.9780	289	0.1971	
				$A_3 = 0.0764 \pm 0.0033$ $E_3 = 29793 \pm 193$ $n_3 = 1.115 \pm 0.069$	0.9992	328	0.2524	
4	0.8	475	0.9917	$A_1 = 3.9783\ 10^8 \pm 2.8589\ 10^7$ $E_1 = 113993 \pm 3156$ $n_1 = 1.252 \pm 0.030$	0.9930	238	0.1993	2.47
				$A_2 = 2.2415\ 10^{10} \pm 3.5975\ 10^9$ $E_2 = 144280 \pm 7914$ $n_2 = 1.067 \pm 0.048$	0.9758	290	0.1945	
				$A_3 = 0.2071 \pm 0.0111$ $E_3 = 34649 \pm 250$ $n_3 = 1.155 \pm 0.080$	0.9990	336	0.2540	

Run	p (MPa)	T_{peak} (ºC)	R^2_{adj} of peak fit	Kinetic parameters: A_i (s^{-1}); E_i (J mol^{-1}); n_i.	R^2_{adj} of NLLS fit	T_{max} for the calculated peaks(ºC)	Contribution to the weight loss (c_i)	Fit (%)
7	0.8	475	0.9898	$A_1 = 1.2609\ 10^8 \pm 7.7907\ 10^7$ $E_1 = 109690 \pm 2710$ $n_1 = 1.274 \pm 0.027$	0.9943	238	0.1975	2.78
				$A_2 = 2.1961\ 10^{10} \pm 3.553\ 10^9$ $E_2 = 144825 \pm 8001$ $n_2 = 1.046 \pm 0.049$	0.9766	289	0.1804	
				$A_3 = 0.1006 \pm 0.0049$ $E_3 = 34649 \pm 250$ $n_3 = 1.121 \pm 0.077$	0.9990	332	0.2648	
6	1.5	400	0.9879	$A_1 = 3.0604\ 10^7 \pm 1.8625\ 10^6$ $E_1 = 110557 \pm 2826$ $n_1 = 1.255 \pm 0.028$	0.9940	271	0.2046	2.97
				$A_2 = 4.3976\ 10^{11} \pm 1.0920\ 10^{11}$ $E_2 = 167467 \pm 13083$ $n_2 = 0.9029 \pm 0.059$	0.9553	320	0.1624	
				$A_3 = 1.2036 \pm 0.1994$ $E_3 = 41864 \pm 778$ $n_3 = 1.110 \pm 0.021$	0.9933	332	0.2790	
2	1.5	550	0.9885	$A_1 = 1.4299\ 10^8 \pm 1.0540\ 10^7$ $E_1 = 115006 \pm 3394$ $n_1 = 1.229 \pm 0.031$	0.9927	262	0.2328	2.94
				$A_2 = 3.4011\ 10^{10} \pm 6.2018\ 10^9$ $E_2 = 153124 \pm 9440$ $n_2 = 1.105 \pm 0.055$	0.9705	315	0.2096	
				$A_3 = 0.0618 \pm 0.0017$ $E_3 = 29870 \pm 132$ $n_3 = 1.111 \pm 0.047$	0.9996	362	0.3089	

Caption for Figures

Fig.1. TGA weight-loss curves for the replicated centre point data (T_{peak} = 475 ºC; p = 0.8 MPa).

Fig. 2. Contour plot for the response surface model given in equation 2 (response variable: y_{char}).

Fig. 3. Contour plot for the response surface model given in equation 3 (response variable: y_{FC}).

Fig. 4. Contour plot for the response surface model given in equation 4 (response variable: T_{max}).

Fig. 5. Normal Q-Q plots for the residuals: (a), y_{char}; (b), y_{FC}; (c), T_{max}.

Fig. 6. DTG simulation results for experiment #3 (p = 0.1 MPa; T_{peak} = 550 °C). Solid line corresponds to the calculated –DTG signal for each pseudo-component; bold solid line is the cumulative calculated signal; and (○), are the experimental –DTG values.

Fig. 7. Comparison of –DTG curves for experiments conducted at different pressures: (solid line), run #5 at 0.1 MPa; (○), run #1 at 0.8 MPa; and (■), run #6 at 1.5 MPa.

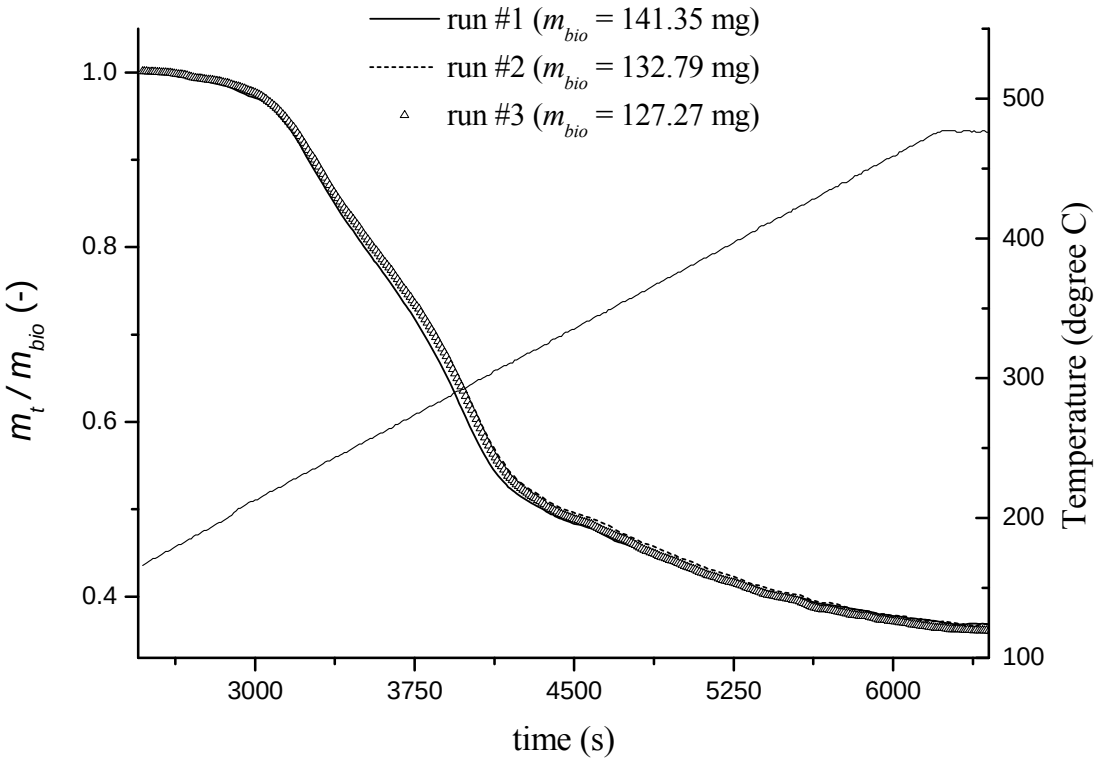

Fig. 1. TGA weight-loss curves for the replicated centre point data (T_{peak} = 475 ºC; p = 0.8 MPa).

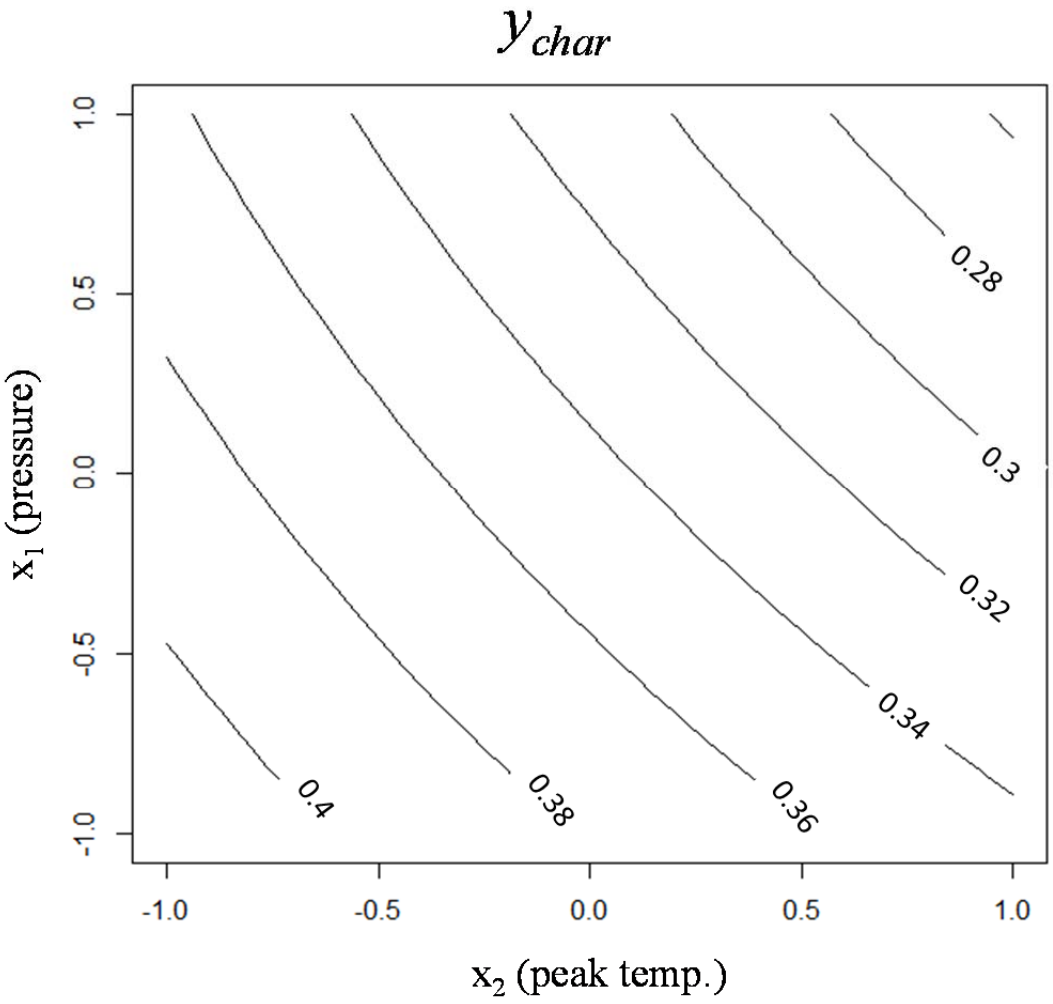

Fig. 2. Contour plot for the response surface model given in equation 2 (response variable: y_{char}).

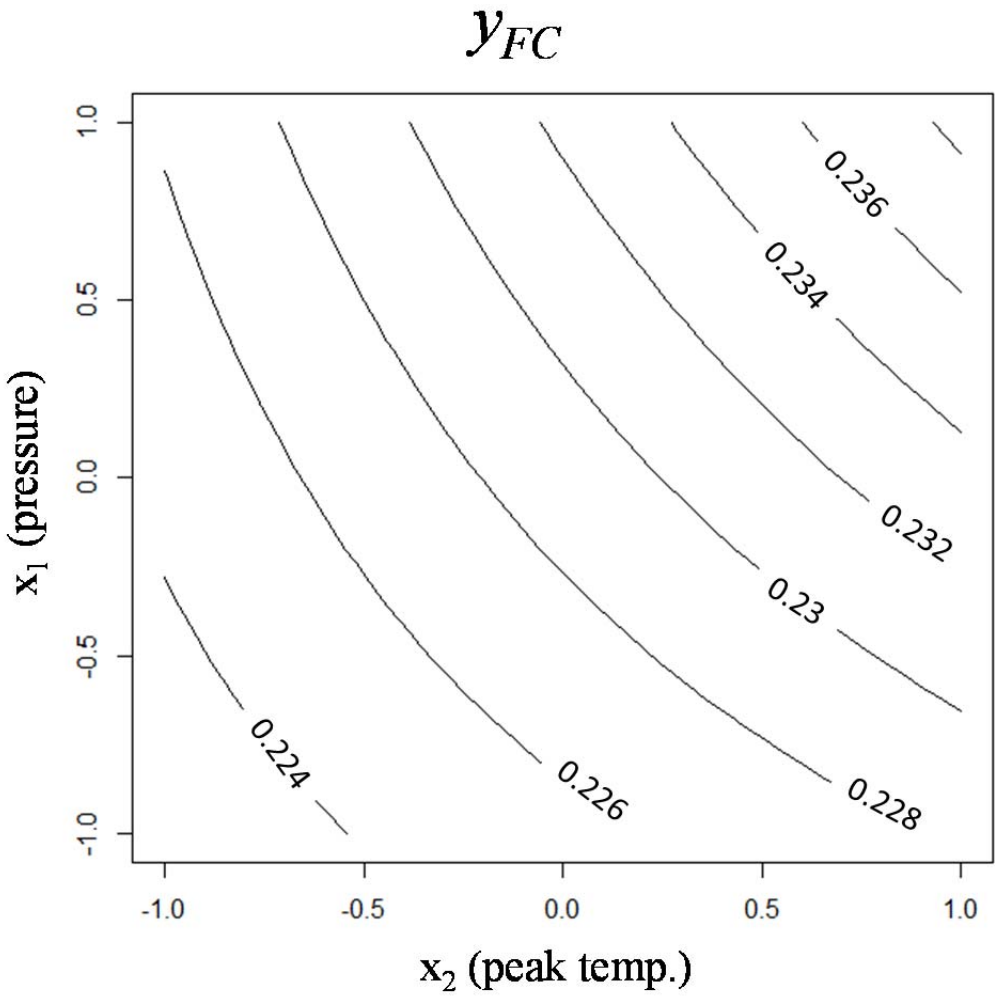

Fig. 3. Contour plot for the response surface model given in equation 3 (response variable: y_{FC}).

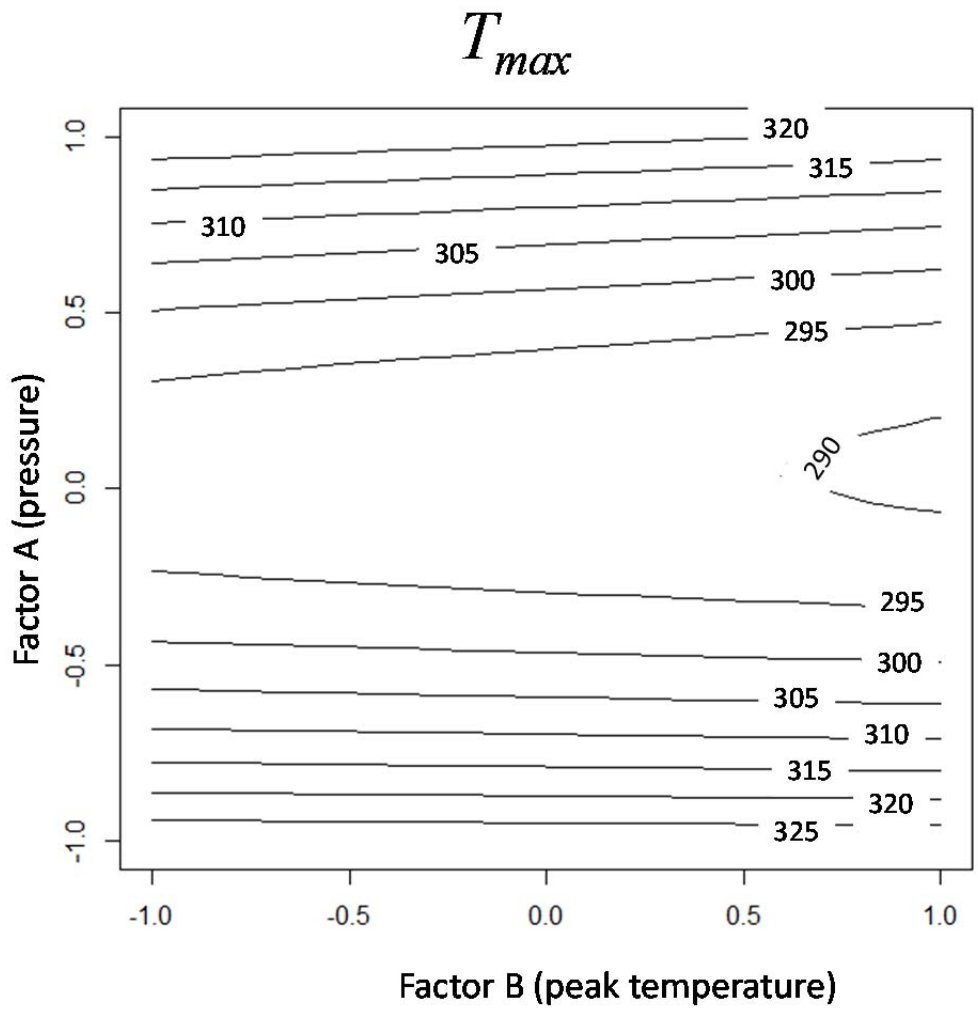

Fig. 4. Contour plot for the response surface model given in equation 4 (response variable: T_{max}).

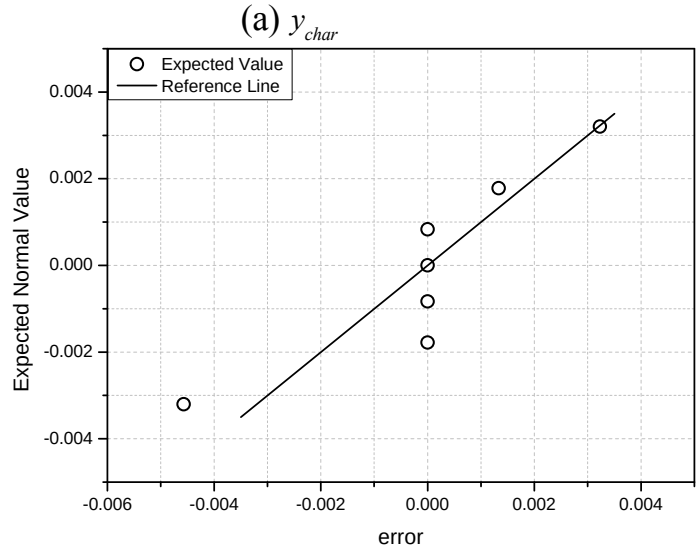

1

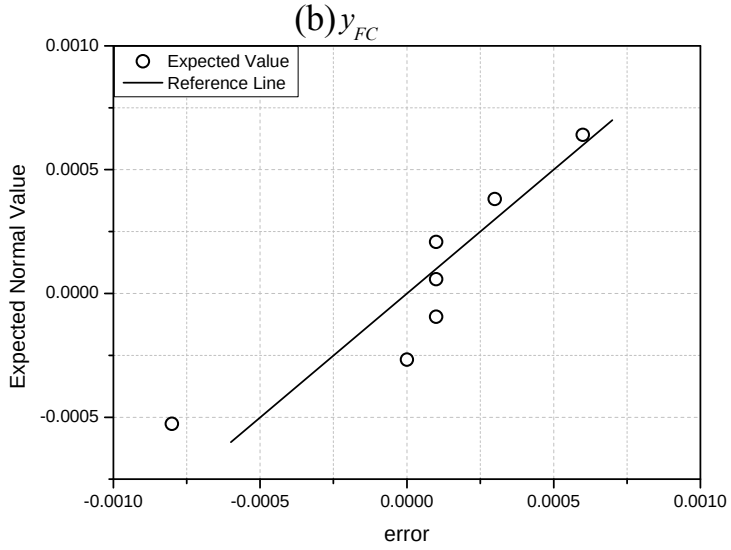

2

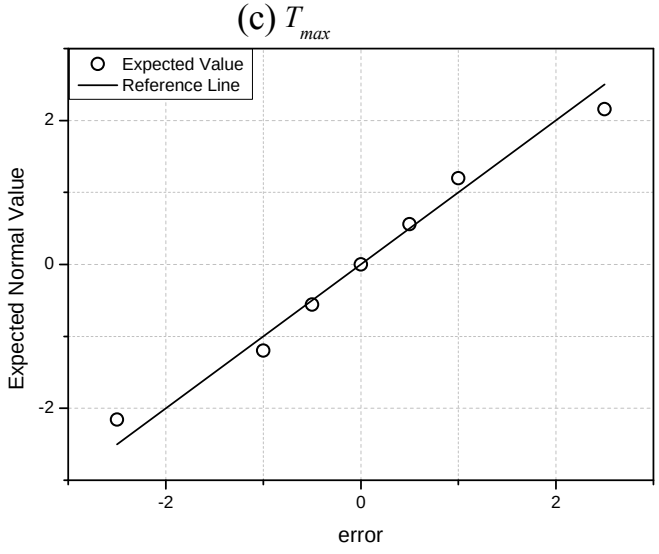

3

4 **Fig. 5**. Normal Q-Q plots for the residuals: (a), y_{char}; (b), y_{FC}; (c), T_{max}.

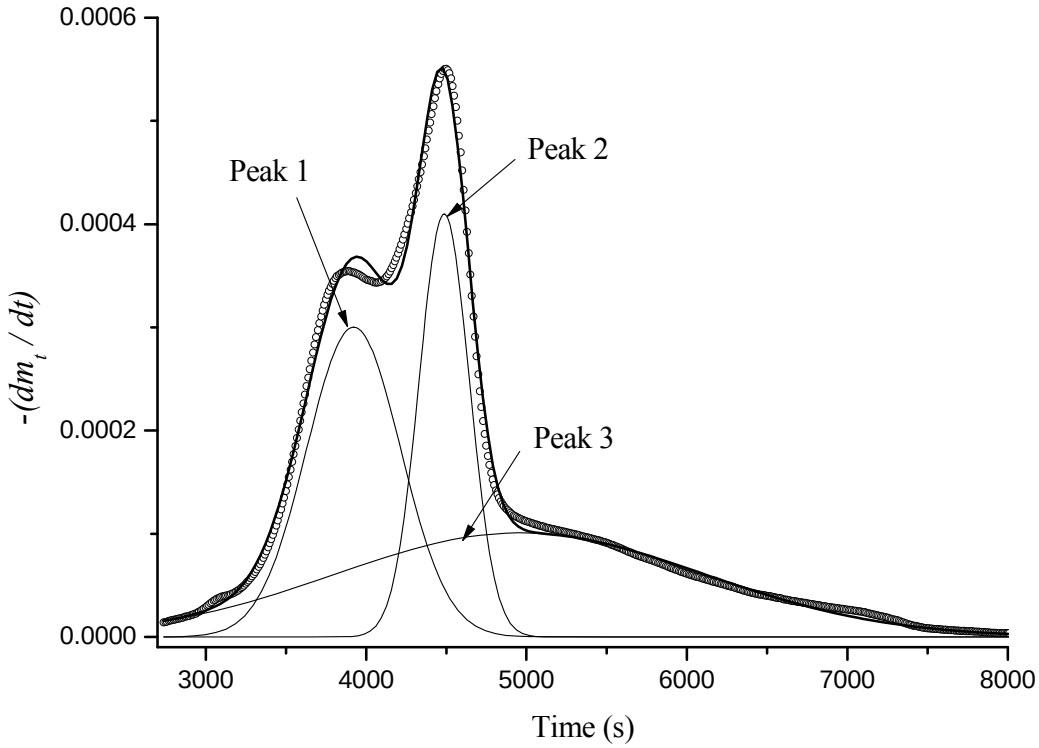

Fig. 6. DTG simulation results for experiment #3 (p = 0.1 MPa; T_{peak} = 550 °C). Solid line corresponds to the calculated –DTG signal for each pseudo-component; bold solid line is the cumulative calculated signal; and (○), are the experimental –DTG values.

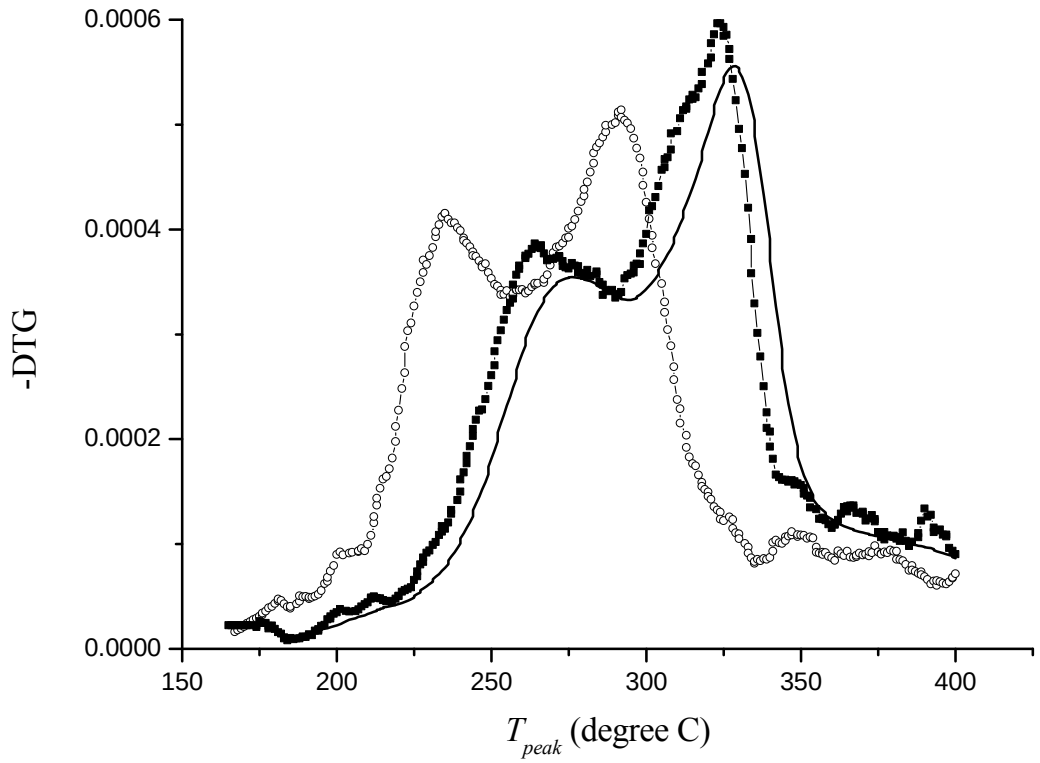

Fig. 7. Comparison of –DTG curves for experiments conducted at different pressures: (solid line), run #5 at 0.1 MPa; (○), run #1 at 0.8 MPa; and (■), run #6 at 1.5 MPa.